



## RESEARCH ARTICLE

10.1002/2015WR016966

## Key Points:

- Floods in the subhumid Pampas are sporadic but can last several years
- Connectivity between surface and belowground water shapes flood dynamics
- Plant transpiration from nonflooded areas could significantly regulate floods

## Supporting Information:

- Supporting Information S1

## Correspondence to:

S. Kuppel,  
skuppel1@gmail.com

## Citation:

Kuppel, S., J. Houspanossian, M. D. Nasetto, and E. G. Jobbágy (2015), What does it take to flood the Pampas?: Lessons from a decade of strong hydrological fluctuations, *Water Resour. Res.*, 51, 2937–2950, doi:10.1002/2015WR016966.

Received 22 JAN 2015

Accepted 2 APR 2015

Accepted article online 6 APR 2015

Published online 26 APR 2015

## What does it take to flood the Pampas?: Lessons from a decade of strong hydrological fluctuations

S. Kuppel<sup>1</sup>, J. Houspanossian<sup>1</sup>, M. D. Nasetto<sup>1</sup>, and E. G. Jobbágy<sup>1</sup>
<sup>1</sup>Grupo de Estudios Ambientales, IMASL-CONICET/Universidad Nacional de San Luis, San Luis, Argentina

**Abstract** While most landscapes respond to extreme rainfalls with increased surface water outflows, very flat and poorly drained ones have little capacity to do this and their most common responses include (i) increased water storage leading to rising water tables and floods, (ii) increased evaporative water losses, and, after reaching high levels of storage, (iii) increased liquid water outflows. The relative importance of these pathways was explored in the extensive plains of the Argentine Pampas, where two significant flood episodes (denoted FE1 and FE2) occurred in 2000–2003 and 2012–2013. In two of the most flood-prone areas (Western and Lower Pampa, 60,000 km<sup>2</sup> each), surface water cover reached 31 and 19% during FE1 in each subregion, while FE2 covered up to 22 and 10%, respectively. From the spatiotemporal heterogeneity of the flood events, we distinguished slow floods lasting several years when the water table is brought to the surface following sustained precipitation excesses in groundwater-connected systems (Western Pampa), and “fast” floods triggered by surface water accumulation over the course of weeks to months, typical of poor surface-groundwater connectivity (Lower Pampa) or when exceptionally strong rainfalls overwhelm infiltration capacity. Because of these different hydrological responses, precipitation and evapotranspiration were strongly linked in the Lower Pampa only, while the connection between water fluxes and storage was limited to the Western Pampa. In both regions, evapotranspirative losses were strongly linked to flooded conditions as a regulatory feedback, while liquid water outflows remained negligible.

## 1. Introduction

Flooding is a natural process in flat continental and coastal landscapes, and a key component of the hydrological connectivity ensuring the water-mediated transport of energy, matter, and living organisms, and ecological processes and features [Heiler *et al.*, 1995; Pringle, 2001]. Yet, because they also affect infrastructure and agricultural production ecosystems (e.g., crops and pastures), flood events are commonly seen as a hazard, potentially jeopardizing local economies, transportation networks, and human life [de Loe, 2000; Viglizzo and Frank, 2006].

Very flat sedimentary regions with low topographic gradients and poorly developed drainage networks preclude the surface drainage of excess water (i.e., precipitation inputs exceeding evapotranspiration) often have relatively stagnant hydrological systems that lead to shallow water tables and long-lasting floods [Fan *et al.*, 2013]. While in well-drained and sloped landscapes enhanced liquid water outflow is the most immediate response to rainfall excesses, stagnant systems are more likely to respond with (i) increased water storage leading to rising water tables and floods, (ii) higher evapotranspirative water losses favored by higher water storage and availability and, at very high levels of water storage, (iii) enhanced liquid water outflows favored by the surface water connectivity [Aragón *et al.*, 2010]. The relative importance of these three hydrological pathways significantly determines the timing, duration, and extent of flood episodes, with strong ramifications on ecosystem functioning (e.g., evapotranspiration is linked to primary production), biogeochemical balances (e.g., liquid outflows are associated with nutrient and salt exports), and atmospheric feedbacks (e.g., flooded area affects surface energy exchange processes).

Extended flat landscapes show low horizontal water transport as a result of low surface runoff and slow groundwater fluxes that become dominated by local-to-intermediate-scale flow paths [Tóth, 1963]. Hence, the water balance of these systems is primarily driven by precipitation and evapotranspiration, while the fluxes of groundwater (GW) and its connection with surface water (SW) are highly dependent on the hydraulic conductivity and texture/porosity of soils [Brunke and Gonser, 1997; Ferone and Devito, 2004; Kollet,

2009]. In landscapes with shallow groundwater, the degree of GW-SW coupling affects in turn the generation of flood events and the behavior of regional water storage (response (i) above). High GW-SW coupling will first result in GW recharge until water tables get close enough to the surface to emerge and increase the area of surface water bodies, while low GW-SW coupling will result in a more rapid flooding before infiltration and GW recharge take place. These two idealized extreme responses can be seen as triggering, in the first case, slow flood episodes lagging behind strong rainfall periods, while the second case would cause faster flood appearance and retraction with a notable hysteresis between GW and SW dynamics.

In landscapes that are usually nonflooded, precipitation inputs directly control soil moisture and evapotranspiration through both bare soil evaporation [Chen and Hu, 2004] and plant transpiration [Baldocchi and Xu, 2007; Chen *et al.*, 2008]. Yet, where water tables are shallow soil moisture is also influenced by groundwater dynamics [Kollet, 2009; Soyulu *et al.*, 2011], and this can have positive or negative effects on evapotranspiration rates. Obvious enhancing effects are related to the increased water availability for both direct soil evaporation and plant transpiration. However, inhibiting effects can arise as well if water excesses hinder plant transpiration through waterlogging and root anoxia [Beltrão *et al.*, 1996; Rathore *et al.*, 1998; Noretto *et al.*, 2009], increased soil salinity [Noretto *et al.*, 2013], and die-off or lack of successful establishment of cultivated vegetation [Viglizzo *et al.*, 2009]. The net effect on evapotranspiration will thus depend on vegetation tolerance to salinity and waterlogging, and on the extent to which direct evaporation from moist or waterlogged soils can compensate for reduced transpiration [Moffett *et al.*, 2010]. Although we expect that increased evaporative losses will occur in surface water-covered areas, the surrounding flood-free landscapes of the plains in which water tables are closer to the surface may result in either negative or positive net changes in their evapotranspirative losses. Finally, extreme flooding can favor the coalescence of surface water bodies, triggering long-distance runoff and surface water drainage out of the flooded region (response (iii) above) as more commonly seen in humid sedimentary plains like the Amazon basin [Richey *et al.*, 1989].

The Argentine Pampas are subhumid eolian plains that experience large episodic flood events covering a significant fraction of the landscape for months or even years [Moncaut, 2001; Aragón *et al.*, 2010]. Several regions around the world share this particular topographic/climatic setting, including the Pantanal (Brazil) [Hamilton, 2002], the Orinoco Llanos (Colombia and Venezuela) [Hamilton *et al.*, 2004], the plains of Manitoba and Saskatchewan (Canada) [Jobbágy *et al.*, 2008], the Great Plains of Hungary [Jobbágy *et al.*, 2008], and Western Siberia [Biancamaria *et al.*, 2009]. Extending over more than 600,000 km<sup>2</sup>, the Pampas are mostly covered by annual crops that have displaced cultivated pastures and native grasslands [Hall *et al.*, 1992; Viglizzo and Frank, 2006; Baldi and Paruelo, 2008]. However, the reciprocal influences of land use and environmental hazards, such as floods, have hindered a harmonious combination between ecosystem conservation, human well-being, and efficient farming in this highly productive region [Viglizzo *et al.*, 2009; Noretto *et al.*, 2009, 2012]. As the agricultural use of these arable lands is expected to further intensify in response to increasing global food demand and trade [Paruelo *et al.*, 2005], careful land management strategies must consider the peculiar hydrological behavior of very flat regions.

The understanding of flood dynamics at large spatial and temporal scales in extremely flat sedimentary regions like the Pampas is still in its early stages [Viglizzo *et al.*, 2009; Aragón *et al.*, 2010]. The continuous emergence and improvement of remote-sensing tools has allowed a more systematic detection of floods and surface waters dynamics [Brakenridge, 2014]. In a portion of the Western Pampa, a first attempt that combined surface water area, level and stock estimates together with precipitation data provided the first quantitative characterization of a single flood cycle (1996–2005) and its associated water balance shifts [Aragón *et al.*, 2010]. Yet, the yearly resolution and limited temporal and spatial extent of this study did not permit evaluation of the timing of floods in response to extreme rainfall episodes, to compare different subregions of the Pampas or distinct flooding cycles, or to ultimately assess the relative importance of the three hydrological responses (i, ii, and iii). In this study, we characterize the dynamics of floods throughout the entire Pampas region of Argentina for a period of nearly 14 years that encompassed at least two major flooding cycles. Based on multiple remote sensing tools, we link these floods to water inputs (precipitation), outputs (evapotranspiration), and storage (total water mass and groundwater levels) to evaluate to what extent slow, groundwater-driven floods or fast, surface water-driven floods prevail. We also explore the relative importance of landscape water storage (i), evapotranspiration (ii) and surface drainage (iii) in balancing water excesses in the region.

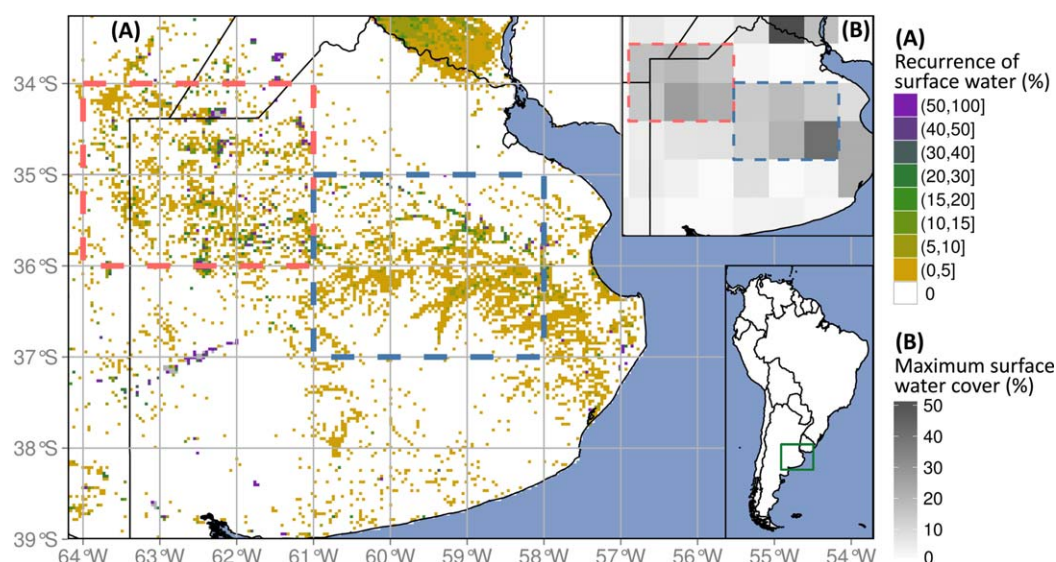


**Figure 1.** (a) Recurrence of surface water cover in the Argentine Pampas at  $500 \times 500 \text{ m}^2$  resolution, expressed as the relative time span under flooded conditions throughout the period from March 2000 to December 2013. The lowest class corresponds to a permanent absence of flooding, as detected by MODIS. The next highest class includes any pixel covered by water at least in one MODIS period (8 days) and up to 5% of the time (254 days). (b) Maximum surface water cover (SWC) at GRACE resolution ( $1^\circ \times 1^\circ$ ) during the same time period. The focus regions are delimited by the dashed red (Western Pampa) and blue (Lower Pampa) lines.

## 2. Material and Methods

### 2.1. Study Region

The study region encompasses most of the Argentine Pampas (Figure 1), a large plain covering approximately  $600,000 \text{ km}^2$  with low elevation ( $<200 \text{ m}$ ) and regional topographic gradients (typically less than a 0.1% slope) [Kruse and Zimmermann, 2002; Viglizzo et al., 2009]. Rainfall in the region decreases from NE to SW, gradually shifting from a relatively even distribution throughout the year to spring-summer-concentrated rain events [Magliano et al., 2014]. Several subregions can be identified in the Pampas, with the most relevant ones in terms of extension and flooding incidence being the Western Pampa and the Lower Pampa (the latter term being preferred to Flooding Pampa—also found in the literature—to avoid confusion). While both regions share a common eolian sedimentary origin [Zárate, 2003], the Western Pampa displays a stronger imprint of wind a deposition on its soils and landforms with widespread dune landscapes, sandy to sandy loam materials, and high density of water bodies in the lower portions of the landscape [Iriondo, 1990; Imbellone and Giménez, 1998]. The Lower Pampa has experienced a strong influence of fluvial forces that reshaped many of the original eolian landforms [Tricart, 1973]. Being further away from the Andean dust sources than the Western Pampa, the Lower Pampa received slightly finer sediments with a higher proportion of silt [Zárate, 2003]. In both regions, subsurface soil horizons with finer texture and secondary calcite formation are common, particularly in lowlands, resulting from illuviation of current and past soil formation cycles, and the spatial extension, thickness and impermeability of these soil horizons is higher in the predominant natric soils of the Lower Pampa [Kröhling, 1999]. The stream and river network in both regions is very poorly developed [Drago and Iriondo, 2004], yet the Lower Pampa shows more permanent water courses, particularly the lower leg of the Salado River that flows into the Atlantic Ocean. Due to a higher proportion of waterlogged and salt-affected soils [Lavado and Taboada, 1988], the Lower Pampa has a lower fraction of its territory devoted to annual crop cultivation than does the Western Pampa [Baldi and Paruelo, 2008].

### 2.2. Remote Sensing of Surface Water Cover

The surface water coverage data were estimated at  $500 \times 500 \text{ m}^2$  resolution with a temporal resolution of 8 days, from 6 March 2000 to 27 December 2013, using the scenes h13v12 and h12v12 of the standard black-sky shortwave albedo product from the MODIS BRDF/albedo product (MCD43A) [Lucht et al., 2000; Schaaf et al., 2002]. Based on a reference water albedo value of 0.06 for solar elevation angles greater than  $30^\circ$  [Gao et al., 2006], which is much lower than the albedo of the typical land cover in the landscape

(grasslands, crops, and fallow lands) [Loarie *et al.*, 2011; Gao, 2005], we applied a simple observational threshold criterion, fixed to 0.09, below which each pixel is considered as covered by water. The MODIS-derived estimate of water-covered pixels was also spatially aggregated to provide the surface water cover (SWC), expressed in percentage of the corresponding area. To improve the accuracy of our SWC estimate, we calibrated our estimates performed in the two focus regions, using LANDSAT data with higher resolution in the same fashion as Arag3n *et al.* [2010] from 2000 to 2011 (see supporting information Text S1).

### 2.3. Other Data Sources and Analysis

The terrestrial water storage (TWS), which is the total vertically integrated water stored above and below the Earth's surface, is provided by the Gravity Recovery And Climate Experiment (GRACE) land data [Swenson and Wahr, 2006; Landerer and Swenson, 2012]. We used the three RL05 solutions releases of the  $1^\circ \times 1^\circ$  near-monthly products from April 2002 to December 2013, provided by the Center for Space Research at the University of Texas at Austin (CSR), the Jet Propulsion Laboratory (JPL), and the German Research Centre for Geosciences (GFZ), to which were applied the scaling factors (provided along with the data sets) compensating for signal modification from sampling and post processing of the original data [Landerer and Swenson, 2012]. Finally, we averaged the three data sources to derive a mean TWS record—then spatially aggregated over both focus regions, as this approach allows reducing the noise within the available gravity field solutions [Sakumura *et al.*, 2014]. Note that the two 60,500 km<sup>2</sup> wide focus regions (see section 3.1) are smaller than the characteristic GRACE footprint (200,000 km<sup>2</sup>) [Longuevergne *et al.*, 2010], calling for a cautious, somewhat qualitative interpretation of the TWS variation and its relation with the other components of the water cycle.

The Tropical Rainfall Measuring Mission (TRMM) provides estimates of precipitation based on remote-sensing observations, covering a global belt (180°W–180°E) between latitudes 50°S and 50°N [Kummerow *et al.*, 1998]. We used the TRMM Multisatellite Precipitation Analysis (TMPA) product generated with version 7 of the 3B42 algorithm, which incorporates a post real-time calibration and merging with monthly rain gauge data [Huffman *et al.*, 2007, 2010]. The 3B42V7 precipitation estimates, originally with 3 h and  $0.25^\circ \times 0.25^\circ$  resolution, were aggregated to daily data for the period covering 1 March 2000 to 31 December 2013. We evaluated the accuracy of these estimates, finding good agreement with in situ precipitation measurements (see supporting information Figure S2). Evapotranspiration (ET) was estimated from an empirical formula derived from the methodology of Di Bella *et al.* [2000], calibrated for the Pampas

$$ET = \frac{-88.3439 + 1.77636 \cdot (0.02 \cdot T_s - 273) + 286.406 \cdot NDVI}{30}, \quad (1)$$

expressed in millimeters per day with resolutions of 8 days and  $1 \times 1$  km<sup>2</sup>.  $T_s$  is the level-3 MODIS daytime land surface temperature in Kelvin (MOD11A2 product), and NDVI is the Normalized Difference Vegetation Index derived from the surface reflectance bands of the MOD09Q1 product. This ET estimate was preferred to the MODIS evapotranspiration product (MOD16A2) [Mu *et al.*, 2011] because the former compared much better to ET values brought by other independent studies [e.g., Noisetto *et al.*, 2015] than the MODIS-based ET did, as it significantly underestimates evapotranspiration in the Pampas region. Importantly, it should be kept in mind that the ET estimate used in this study was only applied in nonflooded areas, with water-covered pixels being excluded from regional averaging.

Lastly, an estimate of monthly groundwater depth (GWD) covering the 2000–2013 time period was reconstructed at the regional scale based on the long-term records available at six sites (Table 1). Because of the location of the monitoring wells, the regional GWD estimate is only considered representative of the Western Pampa, and therefore used for the analysis of this subregion alone. To this end, we used as primary information the GWD monthly variation, given that all sites did not share the same measurement periods and dates, and that the absolute levels of GWD are strongly dependent on the elevation and location of each well in the local landscape (valley, hilltop, etc.), but their temporal level shifts are not and display similar patterns across sites. At each site, GWD variation rates from one record date to the subsequent one were calculated and converted to monthly rates, excluding any intervals longer than 2 months. For each month of the calendar from March 2000 to December 2013, GWD variation rates were averaged across sites to generate a unique time series. Finally, the regional absolute GWD time series was obtained by propagating the regionally averaged GWD variation rate from April 2000 backward (to March 2000) and forward (until December 2013), taking the cross-site-averaged monthly GWD at this date as a reference since all sites have



**Table 1.** Study Sites Used for Long-Term Groundwater Level Measurement (2000–2013)<sup>a</sup>

Site	Longitude (°)	Latitude (°)	Elevation (m)	Wells
Catrillo	−63.45	−36.40	131	3
General Pico (Línea 1)	−63.73	−35.68	134	7
Intendente Alvear	−63.70	−35.31	131	16
La Paz	−61.86	−36.50	117	1
Quemú Quemú	−63.58	−36.05	121	3
Speluzzi	−63.80	−35.48	147	7

<sup>a</sup>For each site, the name, geographic coordinates (decimal degrees), elevation (masl), and number of monitoring wells are indicated.

a recorded GWD value then. Note that a similar procedure had been applied beforehand across the measurement wells of each site—except for La Paz site where there was only one well, so as to avoid giving too much weight to sites having a large number of wells (Table 1).

### 3. Results

#### 3.1. Spatial Distribution

While permanent water bodies were very scarce in the Pampas, intermittent ones (i.e., flooded areas) were widespread and most abundant in the center-north part of the Western Pampa, and in the Salado River basin in the Lower Pampa (Figure 1a). A few large areas with near-permanent water coverage were identified, including the Guaminí lagoons (37.0°S, 62.5°W), Hinojo lagoon (36.0°S, 62.5°W), Picasa lagoon (34.3°S, 62.3°W), and Melincue lagoon (33.7°S, 61.5°W) (Figure 1a). A clear WNW-ESE corridor of approximately 700 km, from the western edge of the region to the Atlantic Ocean, encompasses 49,800 km<sup>2</sup> of territory that became flooded at least once (Figure 1a). We focused the rest of the study on two rectangular subregions covering about 60,500 km<sup>2</sup> each and matching GRACE data cells (Figure 1b). In the first one (red

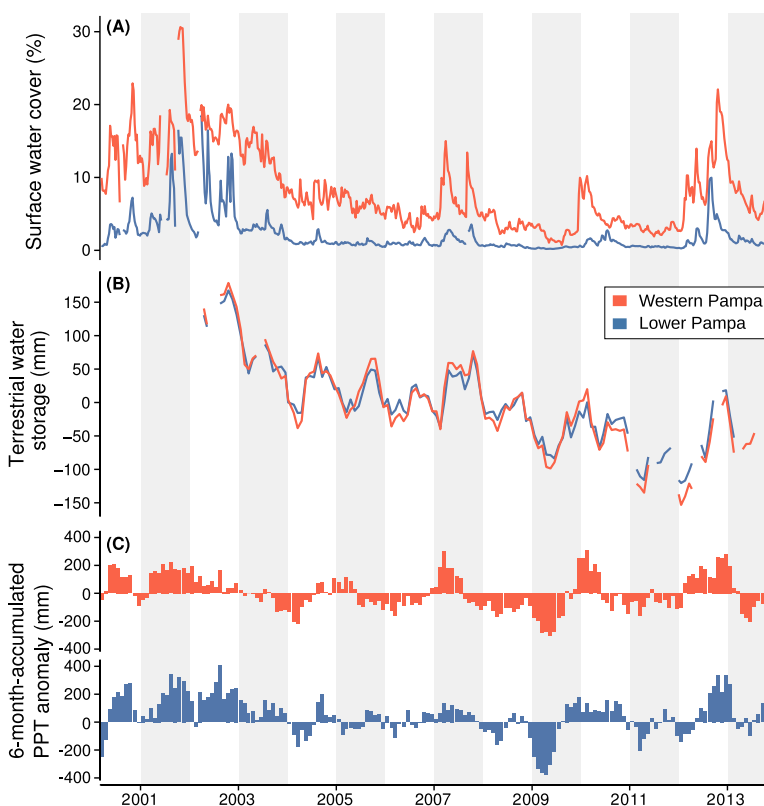


**Figure 2.** Region-averaged (a) surface water cover from 6 March 2000 to 27 December 2013, (b) terrestrial water storage from April 2002 to December 2013, and (c) 6 month-accumulated precipitation (PPT) anomaly (current month and the five preceding ones, using March 2000 to February 2014 as the reference period).

dashed line in Figure 1, 34°S–36°S, 61°W–63°W, hereafter referred to as Western Pampa), 21% of the territory was flooded at least once and up to 5% of the time. In the second focus region (blue dashed line in Figure 1, 35°S–37°S, 58°W–61°W, hereafter referred to as Lower Pampa), 25% of the territory was included in that flooding frequency class. Areas intermittently covered by water more than 5% of the time were much less common, representing only 7.5 and 4.7% of the Western and Lower Pampa, respectively. Note that the lower Paraná River Delta region, although displaying some of the most significant water body occurrence and maximum surface water coverage in the study frame, was excluded from our analysis since it is hydrologically and geologically disconnected from the Pampas and responds to the Paraná River water level fluctuations [see, e.g., Zoffoli *et al.*, 2008].

### 3.2. Temporal Distribution

In the two focus regions two major flood events could be identified since the beginning of the 2000s (Figure 2a). The first event (hereafter FE1) started before 6 March 2000, when MODIS data began to be available, peaking in 2001–2002, and lasting until late 2003. The second event (hereafter FE2) took place over the course of the year 2012 and the first half of 2013. Flood episodes of lesser importance also occurred in 2007 and during the austral summer of 2009–2010, more markedly in the Western Pampa (Figure 2a).

In addition to its duration, FE1 was the most extensive flood episode with water covering up to 30.6 and 18.5% of the Western Pampa and Lower Pampa areas, respectively (Figure 2a). In the Western Pampa, the surface water cover remained above 10% for three and a half years (May 2000 to October 2003), with short drier periods in July 2000 and early 2001. Surface water cover fluctuated around a basal value—by analogy with the stream base flow definition of Arnold and Allen [1999]—of 14–15% from mid-2000 to mid-2003 with a 2 month long peak in late 2001, when the maximum was reached, and later decreased throughout the second half of 2003. The temporal dynamics of FE1 were somewhat different in the Lower Pampa, as there were at least five distinct peaks of surface water coverage above 13% between August 2000 and November 2002, lasting only a few weeks, while basal flood coverage remained around 3% during most of that flooding cycle.

Compared to FE1, FE2 was briefer and less extensive. A first stage could be seen in the Western Pampa with a moderate cover peak in March 2012 (11%), while the maximum flood extent occurred in late October 2012 (22%), before retracting almost completely by the austral winter of 2013. This flooding cycle was even more succinct in the Lower Pampa, starting during the austral fall of 2012, reaching its water cover peak in early September 2012 (10%), and receding by the end of the austral summer in early 2013.

In addition, a significant long-term reduction of the terrestrial water storage was observed following FE1 in the Western and Lower Pampa (Figure 2b), with a respective decline of 162 and 143 mm from maximum annual average values (July–June) in 2002–2003 to minimum values in 2012–2013, in coherence with the larger-scale water depletion reported across the La Plata basin [Chen *et al.*, 2010]. Four stages in the overall water storage trend could be distinguished: (1) a steep decrease at the end and during the aftermath of FE1, by 168 mm (Western Pampa) and 146 mm (Lower Pampa) from April 2002 to April 2004, (2) a somewhat stable trend from 2004 to 2007, (3) a decreasing storage from 2008 to 2011, and finally (4) an increasing trend, by 73 mm (Western Pampa) and 76 mm (Lower Pampa) between December 2011 and December 2013. Also, terrestrial water storage displays a marked and relatively regular seasonal cycle in both regions, with a slightly larger mean amplitude in the Western Pampa (107 mm) than in the Lower Pampa (90 mm).

The time span of both main flood episodes (FE1 and FE2) corresponded to sustained positive precipitation anomalies in both focus regions (Figure 2c). In the Western Pampa, from the beginning of MODIS record to the peak of FE1 the monthly rainfall anomalies summed 453 mm over 20 months, while the 9 month long ascending phase of FE2 corresponded to an accumulated anomaly of 420 mm. In the Lower Pampa, the recorded ascending phase of FE1 until the first large peak took 19 months and coincided with by a summed rainfall anomaly of 548 mm, versus 253 mm within the 7 months of the FE2 buildup. Precipitation excesses of similar magnitude but with shorter duration were visible in the Western Pampa in 2007 and early 2010, when minor flood episodes occurred there. In addition, marked variations of water storage appeared to be a signature of precipitation anomalies (Figures 2b and 2c). In particular, the deep storage valley in 2009 is synchronous with a strong negative accumulated anomaly reaching 305 and 375 mm (i.e., 51 and 63 mm/month on average) in the Western and Lower Pampa, respectively, while a decrease in surface water cover is also noticeable for the Western Pampa (Figure 2a).

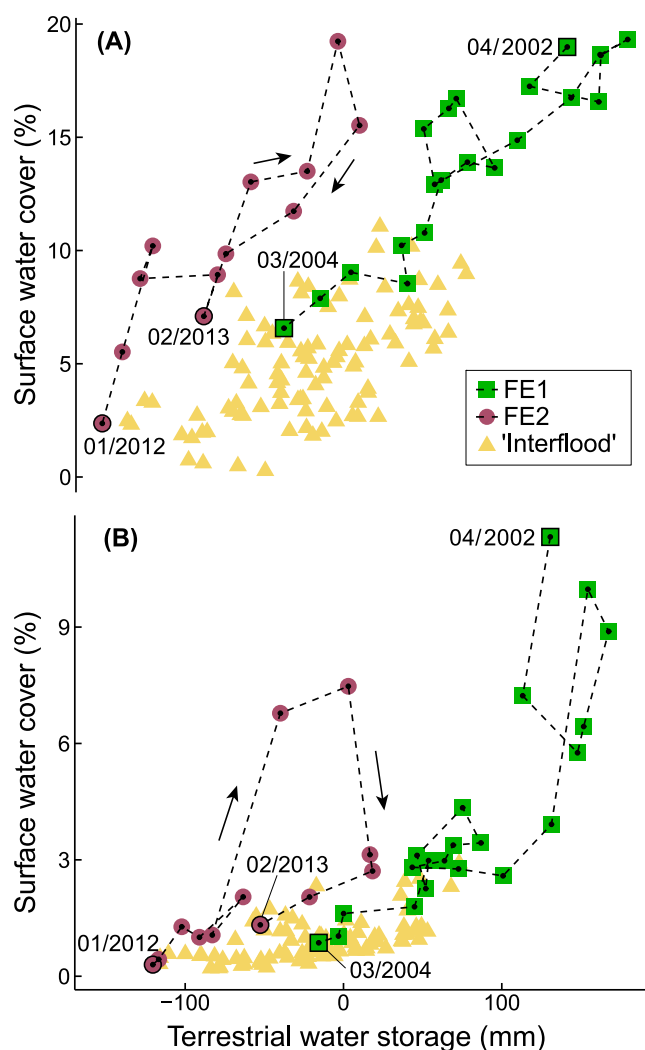


**Figure 3.** Relation between the monthly averaged surface water cover and terrestrial water storage, in (a) the Western Pampa and (b) Lower Pampa. During both flood events FE1 and FE2, the additional dashed lines show the chronological sequence.

ber 2012: similar increase of TWS (40 mm) with a small increase of SWC, (3) September to November 2012 (no TWS record available in October 2012): sharp decrease of SWC down to 3% with a slight increase of TWS, (4) November 2012 to February 2013: progressive decrease of TWS by nearly 70 mm while SWC went back to its “pre-FE2” value.

The two regions thus differ in the much more hysteretic profile of the SWC-TWS relationship in the Lower Pampa, where the flooding extent associated to a given water storage was significantly different between the water-gaining phase and the water-losing phase. For example, in the latter subregion the water storage was roughly the same in August 2012 and in February 2013 ( $TWS < 15$  mm) but in the first case it corresponded to flooded conditions ( $SWC = 6.8\%$ ) that had almost disappeared in the second case ( $SWC = 1.3\%$ ) (Figure 3b). Note that in most cases the visible hysteresis loops are clockwise, meaning that the changes in water storage lag behind those of surface water cover. Finally, in both regions there is a horizontal displacement of the TWS-SWC relationship between the cloud of points corresponding to FE1 and that encompassing FE2 (Figure 3). This TWS offset of nearly 100 mm confirms that less water storage was necessary to cause FE2 than FE1, as could be inferred from Figure 2.

### 3.4. Regional Water Cycles

The correlation analysis between the different components of the water cycle provides insights about the mechanisms triggering flooding in both regions (Table 2 and Figure 4). In the Western Pampa there was a

### 3.3. Water Storage and Floods

The relation between the monthly averaged water-covered area and the total terrestrial water content showed significant differences between subregions and flooding cycles (Figure 3). In the Western Pampa, during both the retraction of FE1 and the full cycle of FE2, it appears that SWC changed somewhat linearly with TWS (Figure 3a), with respective Pearson's  $R^2$  equal to 0.82 and 0.79 ( $p < 0.001$ , not shown). In the Lower Pampa, the poorer linear fit of the TWS-SWC relationship during FE1 and FE2 ( $R^2 = 0.68$  and  $R^2 = 0.41$ , respectively,  $p < 0.05$ , not shown) is significantly improved using an exponential regression ( $R^2 = 0.83$  and  $R^2 = 0.66$ , respectively,  $p < 0.005$ , not shown), suggesting a more time-segmented behavior, with possible threshold-driven water dynamics (Figure 3b). Indeed, a two-step succession could be noticed in the latter subregion during FE1: (1) no significant change of TWS over the course of 2002 when SWC was decreasing threefold (from 11.3 to 3.9%), (2) TWS started to decrease notably from January 2003, while SWC shrank from 2.6 to 0.9%, its value as of March 2004. Also, four steps can be identified during the full FE2 cycle in the Lower Pampa: (1) July to August 2012: sharp increase of SWC from 1% to almost 7% paralleled by a 40 mm increase of TWS, (2) August to September

**Table 2.** Spearman's Rank Correlation Factor Between Annual Quantities (July–June) From 2000–2001 to 2012–2013<sup>a</sup>

Pair of Variables	Western Pampa	Lower Pampa
SWC/TWS	0.645	<b>0.755</b>
SWC/ $\Delta$ TWS	0.164	−0.073
SWC/PPT	0.423	0.599
SWC/ET	<b>0.890</b>	<b>0.852</b>
SWC/PPT-ET	0.028	0.401
TWS/PPT	−0.136	0.136
TWS/ET	<b>0.745</b>	0.518
TWS/PPT-ET	−0.427	−0.218
$\Delta$ TWS/PPT	0.582	0.309
$\Delta$ TWS/ET	0.091	0.200
$\Delta$ TWS/PPT-ET	0.509	0.345
PPT/ET	0.401	<b>0.797</b>

<sup>a</sup>Significance against the null hypothesis is indicated at  $p < 0.1$  (italic) and  $p < 0.01$  (bold).

positive but weak association of precipitation to changes in total water storage, a mild coupling between surface and total water stocks, and a strong association of evapotranspiration to water stocks but none to precipitation (Table 2 and Figure 4). This suggests that this hydrological system has a relatively weak, perhaps lagged or cumulative, response to rainfall, while evapotranspiration depends much more on soil water storage than rainfall. Water balance regulation there most likely follows a path involving water accumulation/depletion (response pathway (i), see section (1) and, with a certain lag, increased/

decreased evapotranspirative losses (pathway (iii)), respectively. Moreover, the robust coupling between total water storage and the groundwater level in the Western Pampa (Figure 5a) would suggest that belowground compartments were the main drivers of the TWS dynamics, at least outside of flood events, and that surface dynamics were linked to those of groundwater. This hypothesis is supported by the fact that the evolution of the surface water bodies in the Western Pampa was strongly linked to groundwater depth during the whole study period, although the relationship substantially changed after 2011 (Figure 5b). Indeed, surface water cover showed a steeper response to phreatic rise and fall (i.e., with negative and positive changes of groundwater depth, respectively) in 2012–2013 than it did over the 11 previous years.

In the Lower Pampa a faster response of evapotranspiration to precipitation excess seemed to take place. By comparison to the Western Pampa, the precipitation was mildly related to surface water cover (instead of total water storage) and strongly to evapotranspiration; the correlation between SWC and TWS was slightly tighter, and total water storage had nil effect on evapotranspiration while surface water cover strongly did (Table 2 and Figure 4). In this case, the response pathway (i) to water excesses would be limited to water accumulation in the shallowest soil layers and at the surface, this storage being itself restricted by rapid evapotranspirative losses to the atmosphere (pathway (ii)). These mechanisms may reflect that the more shallow water table levels of the Lower Pampa are always offering water to plants and hence no particular stimulation of evapotranspiration is seen by increasing water table levels, just the effect of rain. Alternatively, more salty soils and groundwater may prevent water table contribution in the Lower Pampa, making evapotranspiration more responsive to rainfall than to that salty water pool. Moreover, the larger correlation between surface water cover and total water stock in this subregion (Table 2) would not indicate larger water transfer between aboveground and belowground compartments, but rather that occasional surface water bodies play a central role in the water cycle of the Lower Pampa, being the most dynamic

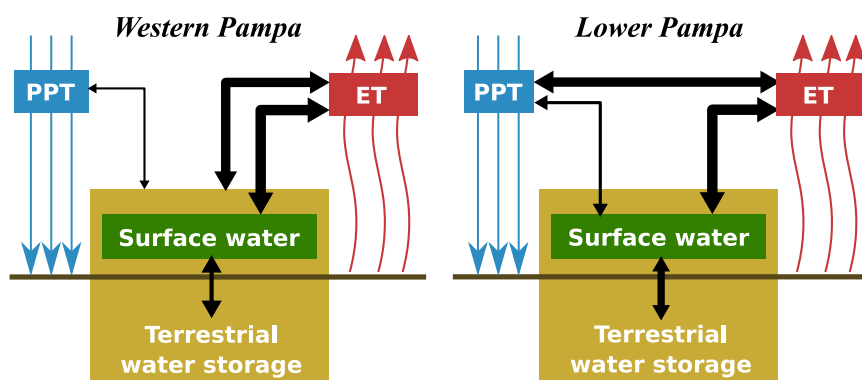


**Figure 4.** Statistically significant connections between the components of the yearly water cycle (left) in the Western Pampa (right) and in the Lower Pampa: precipitation (blue), evapotranspiration (red), surface water cover (green), and terrestrial water storage (gold). The size of the black arrows is proportional to the associated Spearman's rank correlation factor (see Table 2).



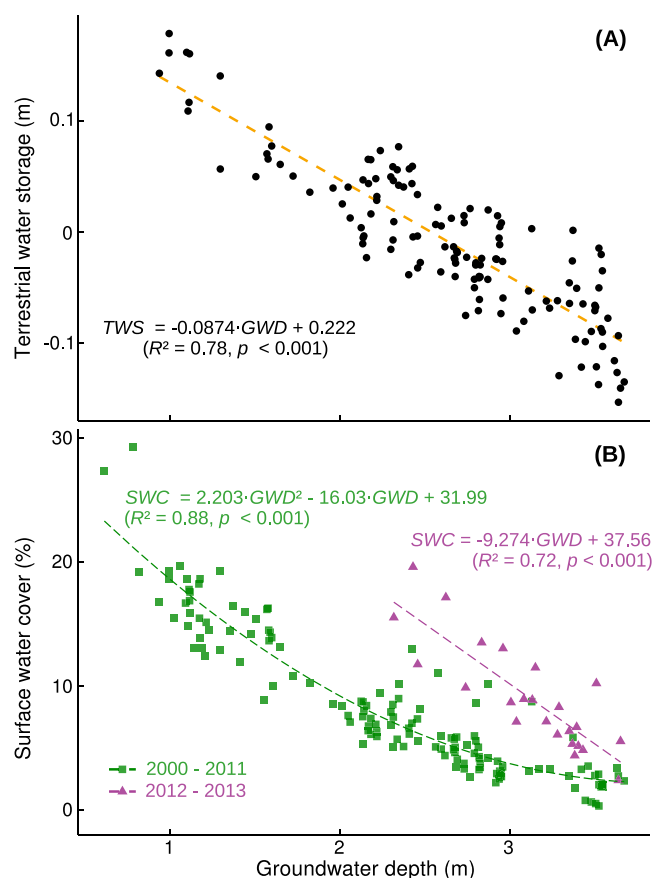


**Figure 5.** Depth to groundwater in the Western Pampa, compared with (a) terrestrial water storage and (b) monthly averaged surface water cover.

[Gabbellone *et al.*, 2005]. Combining flow rate records from stations Junín—where the Salado River exits the Western Pampa—and Guerrero—where in the Salado River exits the Lower Pampa—(P. Garcia, personal communication, 2014) gave a maximum drainage of nearly 15 mm/mo from the Western Pampa and 40 mm/mo from the Lower Pampa in November 2001—the highest recorded values in the available 2000–2004 period, and roughly corresponding to the peak of FE1 in the Western Pampa. Outside these anomalous peaks, the river flow fluctuated around basal flow values corresponding to 3–6 mm/mo. We can thus deduce that liquid water losses in pathway (iii) remain of secondary importance in the water budget of the Argentine Pampas, although they can be dramatically increased at the peak of large flood events.

#### 4. Discussion

Unlike humid sedimentary plains such as the Amazon or the Fly River basins where repeated seasonal water excesses (i.e., precipitation larger than potential evapotranspiration) lead to seasonal flooding cycles every year [Martinez and Letoan, 2007; Swales *et al.*, 1999], the subhumid plains of the Pampas displayed sporadic pulses of floods that lasted several months or even years, followed by several years without flooding conditions. There, the subhumid climatic setting makes water input and output somewhat balanced on a yearly basis. Significant water excesses are relatively unusual, yet they can trigger intense long-lasting flood episodes, as opposed to the more periodical and predictable water balance of the aforementioned humid regions. For this reason, the onset of floods in the Pampas and other flat subhumid regions may represent one of the most serious disturbances of both natural and human systems whose adaptation and adjustment is hampered by the lack of periodicity and hence predictability [Turner *et al.*, 1989].

Two kinds of flood dynamics can be distinguished in the Pampas: slow flood episodes characterized by a moderate surface water cover lasting several years (e.g., most of FE1 in the Western Pampa), and faster

component of the terrestrial water reservoir. This hydrological picture is coherent with the relative decoupling between SWC and TWS at shorter time scales during both flood events in this region (Figure 3b), and the pulse-like profile of surface water as compared to that of the Western Pampa: a larger number of peaks and a lower basal value of SWC (Figure 2a).

The third potential pathway as a response to rainfall excesses, surface water outflows, is difficult to quantify. The definition of the exact limits of the river watershed during flooded periods is very uncertain due to the coalescence of water bodies and small watersheds that would otherwise behave as closed basins, yet a conservative estimate of the basin areas (which yields an exaggerated figure of surface water outflow) can take the rectangular areas used in our study (Figure 1a), the latter being located for their most part in the 150,000 km<sup>2</sup> wide watershed of the Salado river

flood events showing moderate-to-high water cover for weeks to months (e.g., FE1 and FE2 in the Lower Pampa). It is important to highlight that even the faster floods described here are much slower than the typical flashier flood events of just a few days observed in the more sloped territories that cover the majority of the continental surface. The two flood types that we described for the Pampas may occur in combination, as was likely the case during the peak of FE1 in the Western part of the plain in October 2001 (Figure 2a).

The fact that floods showed slower dynamics in the Western Pampa is most likely related to the higher belowground groundwater connectivity, favored by deep sandy sediments, and the lower surface water connectivity, caused by the blockage of surface flow by the wind-shaped relief of this part of the region (Figures 3a and 5) [Viglizzo *et al.*, 2009]. By contrast, the sediments of the Lower Pampa are finer and impermeable layers are more widespread, lowering belowground connectivity. In addition, *Taboada et al.* [2001] showed that the natric soils of the Lower Pampa are subject to swelling-shrinking cycles, resulting from air entrapment and pressure buildup from above (ponding) and below (groundwater head). When connection with the atmospheric pressure is reestablished following the evaporation of ponds (usually in Austral summer), desiccation cracks facilitate groundwater recharge. This particular mechanism may further enhance the vertical decoupling during flood episodes, while also accelerating flood retraction. As initially hypothesized, this low coupling between the aboveground and belowground water compartments not only affected the timing of floods but resulted in hysteretic dynamics in which surface water accumulation preceded groundwater recharge, and the latter could still take place when surface water cover plateaued or even dropped, provided that there were sufficient rainfall inputs (Figure 3b). Note that this sequence of events seems to have even occurred, to a lesser extent, in the Western Pampa during FE2 (Figure 5b), probably because the precipitation anomaly then was twice that of FE1 (Figure 2c). Lastly, note that the surface connectivity in the Lower Pampa is higher due to scarcer local topographic barriers for water flow, yielding an easier coalescence of water bodies during floods (Figure 1a) [Lavado and Taboada, 1988; Chaneton and Lavado, 1996].

Another consequence of this regional difference in flood dynamics is the quality of flooding water. In the Western Pampa, the groundwater-driven floods are likely to bring water with high salt content, causing topsoil salinization after their recession [Taboada *et al.*, 2009]. By contrast, the floods in the Lower Pampa are somewhat similar to a temporary water table above an impervious natric horizon, so that the rain-fed flooding water does not result in topsoil salinization. The latter, when it occurs, originates from the appearance of bare ground surfaces after overgrazing and/or land use changes. From this perspective, floods cannot be considered a disturbance in this region, as they contribute to recover the quality of soils and grasslands [Taboada *et al.*, 1999; Chaneton and Lavado, 1996].

The duration and the possibility to predict floods in the Pampas depend on the dominant response pathway of the hydrologic system and the rate at which large precipitation excesses build up. Whether increased water storage occurs predominantly above (expansion of surface water bodies) or belowground (water table rise and soil moisture increase) dictates how these two compartments interact and to what extent slow or fast flooding patterns prevail. In the Western Pampa a storage anomaly of 100 mm over the arbitrary zeroing of the GRACE records seemed to correspond with sustained flooding (Figure 2b), so that whenever the region approaches this storage the long-lasting and more devastating slow floods should be expected following additional water excess, even if the latter occurs at a slow rate. Below such regional water storages, faster floods can be expected only if additional water excess rapidly builds up, i.e., short and intense positive precipitation anomalies are required. As new flooding episodes unfold and GRACE data availability and processing quality improve, early warning of floods in the Pampas will be not only possible but highly desirable. A more quantitative understanding of storage thresholds and precipitation excess magnitude and buildup rates is still needed to achieve this goal.

From a historical perspective, both FE1 and FE2 corresponded to largely unusual precipitation excesses in both regions: over the last century (1911–2013), 2001 and 2002 were among the five wettest years on record with 200–400 mm above the long-term reference, while the rainfall amount of 2012 was unprecedented (430–580 mm of anomaly) (supporting information Figure S3). Also, in the Western Pampa the 3 year accumulated rainfall anomaly reached 917 mm for the 2000–2002 period, i.e., nearly the average yearly precipitation of the region (not shown). Keeping in mind the limits of this in situ-based analysis (see supporting information section 3), these results seem nonetheless to point to the exceptionality of the rainfall conditions that coincided with FE1 and FE2, and to the fact that precipitations excesses above 200 mm/yr

are likely to result in flooding the Pampas. As mentioned in the previous paragraphs, the magnitude of the flood will notably depend on the pathway taken by the water input, itself influenced by the antecedent water storage in the region and the intensity of the rainfall events.

The most important water output in the Pampas, evapotranspiration (ET), had a more immediate response in the Lower Pampa than in the Western Pampa, as suggested by its much higher correlation with precipitation. In contrast, in the Western Pampa, the effect of evapotranspiration seems to be mediated by water storage, i.e., precipitation excess leads to increased storage and this causes higher evapotranspiration. These differences between subregions may stem from the larger storage capacity of the Western Pampa as compared to the Lower Pampa given its higher soil porosity and depth and large water table fluctuations [Aragón *et al.*, 2010]. Further, the evapotranspiration data used were limited to nonflooded areas which, despite the large flood events, represent by far the largest portion of the studied regions. Therefore, the remarkable correlation between annual mean surface water cover and annual evapotranspiration, both in the Western and Lower Pampa (Table 2), shows that increased regional evaporative losses (pathway (ii)) are associated with flood events. This negative net feedback—in the sense that it tends to self-regulate water excess—is mostly the result of enhanced plant transpiration, to which the ET estimation method that we used is most sensitive, as confirmed by the similar positive correlation between surface water cover and NDVI (not shown). However, this method provides less information about direct soil evaporation. In spite of being a secondary component of ET, direct evaporation could push the negative feedback even more since wetter soils and increased capillary movements of groundwater towards the surface could greatly enhance this flux [Moffett *et al.*, 2010; Shokri and Salvucci, 2011]. Also, our analysis suggests that when the whole region is integrated, the possible positive feedback of waterlogging restricting transpiration in lower landscape positions, as shown by Noretto *et al.* [2009], is likely overwhelmed by the negative feedback of enhanced water supply to plant transpiration mentioned above. A modeling approach could help quantify the relative importance of these ET components in flooded and nonflooded conditions and compare them with the potentially important contribution of evaporation from ephemeral wetlands [Drexler *et al.*, 2004; Mohamed *et al.*, 2012].

Finally, of the three basic hydrological responses to high precipitation anomalies—which include (i) water storage, (ii) evapotranspiration, and (iii) surface water outflow—only the first two were significant in the Pampas. Surface water outflow is surprisingly small in the region as suggested by available flow data for the Salado River (see section 3.4), although lateral surface water movement at local scale can be an important driver of water body coalescence [Aragón *et al.*, 2010]. While this could open avenues for an efficient drainage network reducing the negative impact of flood episodes on human infrastructures while also benefiting—directly and indirectly—agricultural systems, it should be kept in mind, as mentioned in the introduction, that floods are a key driver of the ecological balance of riparian and wetland ecosystems.

## 5. Conclusions

Investigating the flood dynamics in the extensive plains of the Argentine Pampas during the 2000–2013 period, we highlighted two major flood events, in 2000–2003 and 2012–2013, covering up to a quarter of the 120,000 km<sup>2</sup> wide focus area. These floods were subsequent to unusually intense precipitation excesses, and resulted in significantly increased evapotranspirative losses. This feedback might explain the relatively mild change of total water storage during flood events, given that there were negligible horizontal water fluxes. Two types of floods dynamics were identified, and there are not mutually exclusive. Slow floods were primarily driven by large groundwater recharge bringing the water table near to or at the surface, leading to moderate water cover for several years. Faster floods were triggered by surface water accumulation and could produce an extensively flooded landscape for weeks to months. We also found that water dynamics substantially differed between the two halves of the study region (Western Pampa and Lower Pampa), owing to a weak connectivity between aboveground and belowground water compartments in the Lower Pampa as compared to the sandier soils of the Western Pampa. As a result slow, groundwater-driven floods occurred only in the latter region, mostly during the 2000–2003 period. Faster, surface-driven floods were by contrast dominant in the Lower Pampa, but were also found in the Western Pampa when the exceptional rainfall rates overwhelmed the infiltration capacity. In addition, despite the similarities with other large floodplains mentioned in the introduction, the Pampas are distinctively characterized by the

absence of a significant river system, which, associated to extremely low slopes, makes vertical water exchanges the dominant components of the regional water cycle. As a likely consequence, this subhumid region shows a strong sensitivity of floods to positive rainfall anomalies, over the course of weeks to a few months in the Lower Pampa, and at monthly-to-multiannual time scales in the Western Pampa. Finally, the two distinctive hydrological behaviors identified in the Pampas bear consequences for designing efficient flood risk anticipation systems: in addition to near-real-time rainfall and surface water monitoring in the entire region, a more extensive network of phreatic sensors could be of significant added value to warn of the buildup of stored water in the groundwater-connected landscapes such as the highly cultivated Western Pampa.

## Acknowledgments

This work has been supported by the International Development Research Center (project F3), the Agencia Nacional de Promoción Científica y Tecnológica (PRH 27 PICT2008-00187), and the Consejo Nacional de Investigaciones Científicas. The authors would like to thank S. Hamilton, M. Taboada, an anonymous reviewer and the Associate Editor for their valuable comments and suggestions on earlier versions of the manuscript, S. Ballesteros for her help with creating the surface water cover record and the regional water depth times series (both data sets being available upon request to the authors), and E. F. Schibber and C. M. Di Bella for providing the evapotranspiration data set (available upon request). Processing algorithms for GRACE land data (available from <http://grace.jpl.nasa.gov/data/gracemonthlymassgridsland>) were provided by Sean Swenson, and supported by the NASA MEaSUREs Program. Finally, the TRMM 3B42V7 precipitation data set can be retrieved from the Mirador Earth Science Data Search Tool website (<http://mirador.gsfc.nasa.gov>).

## References

- Aragón, R., E. G. Jobbágy, and E. F. Viglizzo (2010), Surface and groundwater dynamics in the sedimentary plains of the Western Pampas (Argentina), *Ecohydrology*, 4(3), 433–447, doi:10.1002/eco.149.
- Arnold, J. G., and P. M. Allen (1999), Automated methods for estimating baseflow and ground water recharge from streamflow records, *J. Am. Water Resour. Assoc.*, 35(2), 411–424.
- Baldi, G., and J. M. Paruelo (2008), Land-use and land cover dynamics in South American temperate grasslands, *Ecol. Soc.*, 13(2), 6.
- Baldocchi, D. D., and L. Xu (2007), What limits evaporation from Mediterranean oak woodlands: The supply of moisture in the soil, physiological control by plants or the demand by the atmosphere?, *Adv. Water Resour.*, 30(10), 2113–2122, doi:10.1016/j.advwatres.2006.06.013.
- Beltrão, J., A. A. Da Silva, and J. B. Asher (1996), Modeling the effect of capillary water rise in corn yield in Portugal, *Irrig. Drain. Syst.*, 10(2), 179–189, doi:10.1007/bf01103700.
- Biancamaria, S., P. D. Bates, A. Boone, and N. M. Mognard (2009), Large-scale coupled hydrologic and hydraulic modelling of the Ob river in Siberia, *J. Hydrol.*, 379(1–2), 136–150, doi:10.1016/j.jhydrol.2009.09.054.
- Brakenridge, G. R. (2014), *Global active archive of large flood events*, Dartmouth Flood Obs., Univ. of Colo. [Available at <http://floodobservatory.colorado.edu/Archives/index.html>.]
- Brunke, M., and T. O. M. Gonser (1997), The ecological significance of exchange processes between rivers and groundwater, *Freshwater Biol.*, 37(1), 1–33, doi:10.1046/j.1365-2427.1997.00143.x.
- Chaneton, E. J., and R. S. Lavado (1996), Soil nutrients and salinity after long-term grazing exclusion in a Flooding Pampa grassland, *J. Range Manage. Arch.*, 49, 182–187, doi:10.2307/4002692.
- Chen, J., C. Wilson, B. Tapley, L. Longuevergne, Z. Yang, and B. Scanlon (2010), Recent La Plata basin drought conditions observed by satellite gravimetry, *J. Geophys. Res.*, 115, D22108, doi:10.1029/2010JD014689.
- Chen, X., and Q. Hu (2004), Groundwater influences on soil moisture and surface evaporation, *J. Hydrol.*, 297(1), 285–300, doi:10.1016/j.jhydrol.2004.04.019.
- Chen, X., Y. Rubin, S. Ma, and D. Baldocchi (2008), Observations and stochastic modeling of soil moisture control on evapotranspiration in a Californian oak savanna, *Water Resour. Res.*, 44, W08409, doi:10.1029/2007WR006646.
- de Loe, R. (2000), Floodplain management in Canada: Overview and prospects, *Can. Geogr.*, 44(4), 355–368, doi:10.1111/j.1541-0064.2000.tb00718.x.
- Di Bella, C. M., C. M. Rebella, and J. M. Paruelo (2000), Evapotranspiration estimates using NOAA AVHRR imagery in the Pampa region of Argentina, *Int. J. Remote Sens.*, 21(4), 791–797, doi:10.1080/014311600210579.
- Drago, E. C., and M. H. Iriondo (2004), The headwater hydrographic characteristics of large plains: The Pampa case, *Ecohydrology. Hydrobiol.*, 4(1), 7–16.
- Drexler, J. Z., R. L. Snyder, D. Spano, U. Paw, and K. Tha (2004), A review of models and micrometeorological methods used to estimate wetland evapotranspiration, *Hydrol. Proc.*, 18(11), 2071–2101, doi:10.1002/hyp.1462.
- Fan, Y., H. Li, and G. Miguez-Macho (2013), Global patterns of groundwater table depth, *Science*, 339(6122), 940–943, doi:10.1126/science.1229881.
- Ferone, J. M., and K. J. Devito (2004), Shallow groundwater–surface water interactions in pond–peatland complexes along a Boreal Plains topographic gradient, *J. Hydrol.*, 292(1), 75–95, doi:10.1016/j.jhydrol.2003.12.032.
- Gabellone, N. A., M. C. Claps, L. C. Solari, and N. C. Neschuk (2005), Nutrients, conductivity and plankton in a landscape approach to a Pampean saline lowland river (Salado River, Argentina), *Biogeochemistry*, 75(3), 455–477.
- Gao, F. (2005), MODIS bidirectional reflectance distribution function and albedo climate modeling grid products and the variability of albedo for major global vegetation types, *J. Geophys. Res.*, 110, D01104, doi:10.1029/2004JD005190.
- Gao, W., Q. Lu, Z. Gao, W. Wu, B. Du, and J. Slusser (2006), Analysis of temporal variations of surface albedo from MODIS, in *Remote Sensing and Modeling of Ecosystems for Sustainability III*, edited by W. Gao and S. L. Ustin, SPIE Optics + Photonics (pp. 62981G–62981G), International Society for Optics and Photonics.
- Hall, A. J., C. M. Rebella, C. M. Ghersa, and J. P. Culot (1992), Field-crop systems of the Pampas, in *Ecosystems of the World (Netherlands)*, Elsevier, Netherlands.
- Hamilton, S. (2002), Comparison of inundation patterns among major South American floodplains, *J. Geophys. Res.*, 107(D20), 8308LBA 5–1–LBA 5–14, doi:10.1029/2000JD000306.
- Hamilton, S., S. Sippel, and J. Melack (2004), Seasonal inundation patterns in two large savanna floodplains of South America: The Llanos de Moxos (Bolivia) and the Llanos del Orinoco (Venezuela and Colombia), *Hydrol. Proc.*, 18(11), 2103–2116, doi:10.1002/hyp.5559.
- Heiler, G., T. Hein, F. Schiemer, and G. Bornette (1995), Hydrological connectivity and flood pulses as the central aspects for the integrity of a river-floodplain system, *Reg. Rivers Res. Manage.*, 11(3–4), 351–361.
- Huffman, G., D. Bolvin, E. Nelkin, D. Wolff, R. Adler, G. Gu, Y. Hong, K. Bowman, and E. F. Stocker (2007), The TRMM multisatellite precipitation analysis (TMPA): Quasi-global multiyear, combined-sensor precipitation estimates at fine scales, *J. Hydrometeorol.*, 8(1), 38–55, doi:10.1175/jhm560.1.
- Huffman, G. J., R. F. Adler, D. T. Bolvin, and E. J. Nelkin (2010), The TRMM multi-satellite precipitation analysis (TMPA), in *Satellite Rainfall Applications for Surface Hydrology*, pp. 3–22, Springer, Netherlands, doi:10.1007/978-90-481-2915-7.



- Imbellone, P., and J. Giménez (1998), Parent materials buried soils and fragipans in northwestern Buenos Aires province, Argentina, *Quat. Int.*, 51–52, 115–126, doi:10.1016/s1040-6182(97)00038-4.
- Iriondo, M. (1990), Map of the South American plains: Its present state, *Quat. South Am. Antarct. Peninsula*, 6, 297–308.
- Jobbágy, E., M. Nasetto, C. Santoni, and G. Baldi (2008), El desafío ecohidrológico de las transiciones entre sistemas leñosos y herbáceos en la llanura Chaco-Pampeana, *Ecol. Austral*, 18(3), 305–322.
- Kollet, S. (2009), Influence of soil heterogeneity on evapotranspiration under shallow water table conditions: Transient stochastic simulations, *Environ. Res. Lett.*, 4(3), 035007, doi:10.1088/1748-9326/4/3/035007.
- Kröhling, D. (1999), Sedimentological maps of the typical loessic units in North Pampa Argentina, *Quat. Int.*, 62(1), 49–55, doi:10.1016/s1040-6182(99)00022-1.
- Kruse, E., and E. Zimmermann (2002), Hidrogeología de grandes llanuras: Particularidades en la llanura pampeana (Argentina), in *Workshop Publication on Groundwater and Human Development*, pp. 2025–2038, La Plata, Argentina.
- Kummerow, C., W. Barnes, T. Kozu, J. Shiue, and J. Simpson (1998), The tropical rainfall measuring mission (TRMM) sensor package, *J. Atmos. Oceanic Technol.*, 15(3), 809–817, doi:10.1175/1520-0426(1998)015<0809:TTRMMT>2.0.CO;2.
- Landerer, F. W., and S. C. Swenson (2012), Accuracy of scaled GRACE terrestrial water storage estimates, *Water Resour. Res.*, 48, W04531, doi:10.1029/2011WR011453.
- Lavado, R., and M. Taboada (1988), Water salt and sodium dynamics in a Natraquoll in Argentina, *Catena*, 15(6), 577–594, doi:10.1016/0341-8162(88)90008-2.
- Loarie, S. R., D. B. Lobell, G. P. Asner, and C. B. Field (2011), Land-cover and surface water change drive large albedo increases in South America, *Earth Interact.*, 15, 1–16, doi:10.1175/2010ei342.1.
- Longuevergne, L., B. R. Scanlon, and C. R. Wilson (2010), GRACE hydrological estimates for small basins: Evaluating processing approaches on the High Plains Aquifer, USA, *Water Resour. Res.*, 46, W11517, doi:10.1029/2009WR008564.
- Lucht, W., C. Schaaf, and A. Strahler (2000), An algorithm for the retrieval of albedo from space using semiempirical BRDF models, *IEEE Trans. Geosci. Remote Sens.*, 38(2), 977–998, doi:10.1109/36.841980.
- Magliano, P., R. Fernández, J. Mercau, and E. Jobbágy (2014), Precipitation event distribution in Central Argentina: Spatial and temporal patterns, *Ecology*, 95, 94–104, doi:10.1002/eco.1491.
- Martinez, J., and T. Letoan (2007), Mapping of flood dynamics and spatial distribution of vegetation in the Amazon floodplain using multi-temporal SAR data, *Remote Sens. Environ.*, 108(3), 209–223, doi:10.1016/j.rse.2006.11.012.
- Moffett, K., A. Wolf, J. Berry, and S. Gorelick (2010), Salt marsh-atmosphere exchange of energy water vapor, and carbon dioxide: Effects of tidal flooding and biophysical controls, *Water Resour. Res.*, 46, W10525, doi:10.1029/2009WR009041.
- Mohamed, Y., W. Bastiaanssen, H. Savenije, B. van den Hurk, and C. Finlayson (2012), Wetland versus open water evaporation: An analysis and literature review, *Phys. Chem. Earth*, 47–48, 114–121, doi:10.1016/j.pce.2011.08.005.
- Moncaut, C. (2001), *Inundaciones y Sequías en la Pampa Bonaerense: 1576–2001*, 102 pp., Editorial El Aljibe, City Bell, Argentina.
- Mu, Q., M. Zhao, and S. W. Running (2011), Improvements to a MODIS global terrestrial evapotranspiration algorithm, *Remote Sens. Environ.*, 115(8), 1781–1800.
- Nasetto, M. D., E. G. Jobbágy, R. B. Jackson, and G. A. Sznaider (2009), Reciprocal influence of crops and shallow ground water in sandy landscapes of the Inland Pampas, *Field Crops Res.*, 113(2), 138–148, doi:10.1016/j.fcr.2009.04.016.
- Nasetto, M. D., E. G. Jobbágy, A. B. Brizuela, and R. B. Jackson (2012), The hydrologic consequences of land cover change in central Argentina, *Agric. Ecosyst. Environ.*, 154, 2–11, doi:10.1016/j.agee.2011.01.008.
- Nasetto, M. D., A. M. Acosta, D. H. Jayawickreme, S. I. Ballesteros, R. B. Jackson, and E. G. Jobbágy (2013), Land-use and topography shape soil and groundwater salinity in central Argentina, *Agric. Water Manage.*, 129, 120–129, doi:10.1016/j.agwat.2013.07.017.
- Nasetto, M. D., R. A. Paez, S. I. Ballesteros, and E. G. Jobbágy (2015), Higher water-table levels and flooding risk under grain vs. livestock production systems in the subhumid plains of the Pampas, *Agric. Ecosyst. Environ.*, 206, 60–70, doi:10.1016/j.agee.2015.03.009.
- Paruelo, J. M., J. P. Guerschman, and S. R. Verón (2005), Expansión agrícola y cambios en el uso del suelo, *Cienc. Hoy*, 15(87), 14–23.
- Pringle, C. M. (2001), Hydrologic connectivity and the management of biological reserves: A global perspective, *Ecol. Appl.*, 11(4), 981–998, doi:10.1890/1051-0761(2001)011[0981:HCATMO]2.0.CO;2.
- Rathore, T. R., M. Z. K. Warsi, N. N. Singh, and S. K. Vasal (1998), Production of maize under excess soil moisture (waterlogging) conditions, in *Proceedings of the 2nd Asian Regional Maize Workshop PACARD*, pp. 23–27, Los Banos, Philippines.
- Richey, J. E., L. A. Mertes, T. Dunne, R. L. Victoria, B. R. Forsberg, A. C. Tancredi, and E. Oliveira (1989), Sources and routing of the Amazon River flood wave, *Global Biogeochem. Cycles*, 3(3), 191–204, doi:10.1029/gb003i003p00191.
- Sakumura, C., S. Bettadpur, and S. Bruinsma (2014), Ensemble prediction and intercomparison analysis of GRACE time-variable gravity field models, *Geophys. Res. Lett.*, 41, 1389–1397, doi:10.1002/2013GL058632.
- Schaaf, C., et al. (2002), First operational BRDF albedo nadir reflectance products from MODIS, *Remote Sens. Environ.*, 83(1–2), 135–148, doi:10.1016/s0034-4257(02)00091-3.
- Shokri, N., and G. Salvucci (2011), Evaporation from porous media in the presence of a water table, *Vadose Zone J.*, 10(4), 1039–1318, doi:10.2136/vzj2011.0027.
- Soylu, M. E., E. Istanbuluoglu, J. D. Lenters, and T. Wang (2011), Quantifying the impact of groundwater depth on evapotranspiration in a semi-arid grassland region, *Hydrol. Earth Syst. Sci.*, 15(3), 787–806, doi:10.5194/hessd-7-6887-2010.
- Swales, S., A. Storey, I. Roderick, and B. Figa (1999), Fishes of floodplain habitats of the Fly River system, Papua New Guinea, and changes associated with El Niño droughts and algal blooms, *Environ. Biol. Fishes*, 54(4), 389–404, doi:10.1023/a:1007474501507.
- Swenson, S., and J. Wahr (2006), Post-processing removal of correlated errors in GRACE data, *Geophys. Res. Lett.*, 33, L08402, doi:10.1029/2005GL025285.
- Taboada, M. A., R. S. Lavado, H. Svartz, and A. M. L. Segat (1999), Structural stability changes in a grazed grassland Natraquoll of the Flooding Pampa of Argentina, *Wetlands*, 19(1), 50–55.
- Taboada, M. A., R. S. Lavado, G. Rubio, and D. J. Cosentino (2001), Soil volumetric changes in natric soils caused by air entrapment following seasonal ponding and water table, *Geoderma*, 101(3), 49–64.
- Taboada, M. A., F. Damiano, and R. S. Lavado (2009), Inundaciones en la Región Pampeana. Consecuencias sobre los suelos, in *Alteraciones de la fertilidad de los suelos: el halomorfismo, la acidez, el hidromorfismo y las inundaciones*, edited by M. A. Taboada and R. S. Lavado, pp. 103–127, Univ. de Buenos Aires, Buenos Aires, Argentina.
- Tóth, J. (1963), A theoretical analysis of groundwater flow in small drainage basins, *J. Geophys. Res.*, 68(16), 4795–4812, doi:10.1029/jz068i016p04795.



- Tricart, J. (1973), *Geomorfología de la Pampa Deprimida: Base para los estudios edafológicos y agronomicos*, vol. xi, 202 pp., Secr. de Estado de Agric. y Ganadería de la Nac., Inst. Nacl. de Tecnol. Agropecuaria, Buenos Aires, Argentina.
- Turner, M., R. Gardner, V. Dale, and R. O'Neill (1989), Predicting the spread of disturbance across heterogeneous landscapes, *Oikos*, 55(1), 121, doi:10.2307/3565881.
- Viglizzo, E. F., and F. C. Frank (2006), Ecological interactions, feedbacks, thresholds and collapses in the Argentine Pampas in response to climate and farming during the last century, *Quat. Int.*, 158(1), 122–126, doi:10.1016/j.quaint.2006.05.022.
- Viglizzo, E. F., E. G. Jobbágy, L. Carreño, F. C. Frank, R. Aragón, L. De Oro, and V. Salvador (2009), The dynamics of cultivation and floods in arable lands of Central Argentina, *Hydrol. Earth Syst. Sci.*, 13(4), 491–502, doi:10.5194/hess-13-491-2009.
- Zárate, M. A. (2003), Loess of southern South America, *Quat. Sci. Rev.*, 22(18), 1987–2006, doi:10.1016/s0277-3791(03)00165-3.
- Zoffoli, M. L., P. Kandus, N. Madanes, and D. H. Calvo (2008), Seasonal and interannual analysis of wetlands in South America using NOAA-AVHRR NDVI time series: The case of the Paraná Delta Region, *Landscape Ecol.*, 23(7), 833–848, doi:10.1007/s10980-008-9240-9.